APPLICATION OF TWO-STEP DECOMPOSITION TO MULTICOMPONENT OCEAN-BOTTOM DATA: THEORY AND CASE STUDY

K.M. SCHALKWIJK, C.P.A. WAPENAAR and D.J. VERSCHUUR

Centre for Technical Geoscience, Laboratory of Seismics and Acoustics, Delft University of Technology, P.O. Box 5046, 2600 GA Delft, Netherlands.

(Received February 17, 1999; revised version accepted June 7, 1999)

ABSTRACT

Schalkwijk, K.M., Wapenaar, C.P.A. and Verschuur, D.J., 1999. Application of two-step decomposition to multicomponent ocean-bottom data: theory and case study. *Journal of Seismic Exploration*, 8: 261-278.

Multicomponent ocean-bottom acquisition, where the particle velocity vector and the pressure are measured (4-C data), enables us to decompose the data. When talking about a decomposition of ocean-bottom data there are two possibilities. An *acoustic* decomposition can be performed just above the ocean-bottom, giving the up- and downgoing pressure fields in the water. Or an *elastic* decomposition can be performed just below the ocean-bottom, in which case the up- and downgoing P- and S-waves are obtained. The latter result can then be used in further processing. The elastic decomposition procedure, based on the wave equation, only requires knowledge of the medium parameters just below the receiver level.

In this paper the decomposition theory is reviewed. From this theory a two-step decomposition procedure is derived, where the up- and downgoing wavefields and the P- and S-waves are decomposed into two separate steps.

Then the decomposition theory is applied to a deep ocean-bottom field dataset. Instead of going from the measured data directly to the end result - up- and downgoing P- and S-waves - a more practical decomposition procedure is proposed here, that uses several intermediate decomposition results before coming to the final result. Each intermediate result allows for the estimation of some unknown parameters. In addition, the quality of the intermediate results can be checked and, if necessary, improved.

KEY WORDS: decomposition, multicomponent, ocean-bottom, converted waves, optimization.

0963-0651/99/$5.00

INTRODUCTION

The aim of the decomposition procedure is to separate the measured data into its up- and downgoing P- and S-wave constituents. Assuming a flat ocean-bottom, for normal incidence (0°) the vertical geophone is sensitive only to P-waves and the horizontal geophone only to S-waves. For oblique angles of incidence, a decomposition becomes necessary if one wants to process the P- and S-waves separately. After migration and inversion of the separated P- and S-wavefields, additional information about the subsurface is expected to be obtained, e.g., better illumination of the layer-structure in gas regions, anisotropy, lithologic parameters (c_P/c_S ratios), porosity, etc. [see for example Hovem et al. (1990); Tatham and McCormack (1991)]. This will not be further discussed in this paper.

Decomposition of ocean-bottom data has been previously discussed by Amundsen and Reitan (1995), Osen et al. (1996) and Donati and Stewart (1996) amongst others, as a modification of schemes by White (1965), Dankbaar (1985), and Wapenaar et al. (1990). The decomposition procedure in essence combines the pressure, horizontal and vertical velocity components after application of the appropriate decomposition operator to each of these components. In order to calculate the operators, the medium parameters just below the receiver level need to be known. This indicates why the application of decomposition to field data is not straightforward; the medium parameters are unknown and due to measurement imperfections (different coupling, impulse response, etc.), the components need to be calibrated to each other before they can be combined.

To tackle these obstacles, the elastic decomposition equations are rewritten in a simpler form by splitting the decomposition into two steps - first a separation of up- and downgoing wavefields, then a separation into P- and S-waves. The two-step decomposition equations will be derived from the elastic one-step decomposition equations, following the derivation for a land acquisition setting in Wapenaar and Haimé (1991). Then an adaptive decomposition scheme [see also Schalkwijk et al. (1998)] that allows estimation of the required quantities from the data itself , will be proposed and tested on a field dataset with an ocean-bottom at approximately 1300 meters depth.

ONE-STEP VERSUS TWO-STEP DECOMPOSITION

In the case of a decomposition at the ocean-bottom there is the choice of performing a decomposition just above the bottom (acoustic decomposition) or just below the bottom (elastic decomposition). In the first case the up- and downgoing pressure wavefields in the water-layer are obtained; the latter case results in the up- and downgoing P- and S-waves just below the receiver level.

The composition and decomposition equations [equations (1) and (2) below] give the relations between the two-way wavefield vectors (in terms of the total particle velocity and traction) and one-way wavefield vectors (acoustically in terms of downgoing and upgoing pressure wavefields, elastically in terms of potentials for downgoing and upgoing P- and S-waves). For laterally invariant media, derivations of the decomposition equations from the elastic wave equation have been given in various publications (Frasier, 1970; Aki and Richards, 1980; Kennett, 1983; Ursin, 1983). When written in the rayparameter-frequency (p,ω) domain the composition/decomposition equations are given by

$$\begin{pmatrix} -\tilde{\boldsymbol{\tau}}_z(z) \\ \tilde{\mathbf{V}}(z) \end{pmatrix} = \begin{pmatrix} \tilde{\mathbf{L}}_1^+(z) & \tilde{\mathbf{L}}_1^-(z) \\ \tilde{\mathbf{L}}_2^+(z) & \tilde{\mathbf{L}}_2^-(z) \end{pmatrix} \begin{pmatrix} \tilde{\mathbf{D}}^+(z) \\ \tilde{\mathbf{D}}^-(z) \end{pmatrix} \tag{1}$$

and

$$\begin{pmatrix} \tilde{\mathbf{D}}^+(z) \\ \tilde{\mathbf{D}}^-(z) \end{pmatrix} = \begin{pmatrix} \tilde{\mathbf{N}}_1^+(z) & \tilde{\mathbf{N}}_2^+(z) \\ \tilde{\mathbf{N}}_1^-(z) & \tilde{\mathbf{N}}_2^-(z) \end{pmatrix} \begin{pmatrix} -\tilde{\boldsymbol{\tau}}_z(z) \\ \tilde{\mathbf{V}}(z) \end{pmatrix}, \tag{2}$$

respectively. Note that only the z-dependency has been written explicitly. Hence, $\tilde{\mathbf{V}}(z)$ stands for $\tilde{\mathbf{V}}(p,z,\omega)$ etc.

In the acoustic case, the traction and particle velocity vectors and the one-way wavefield vectors become scalars

$$\tilde{\tau}_z(z) = -\tilde{P}(z), \quad \tilde{\mathbf{V}}(z) = \tilde{V}_z(z), \tag{3}$$

and

$$\tilde{\mathbf{D}}^+(z) = \tilde{P}^+(z), \quad \tilde{\mathbf{D}}^-(z) = \tilde{P}^-(z), \tag{4}$$

where $\tilde{P}(z)$ is the acoustic pressure at depth level z, $\tilde{V}_z(z)$ the vertical component of the particle velocity and where $\tilde{P}^+(z)$ and $\tilde{P}^-(z)$ represent the downgoing and upgoing pressure wavefields, respectively.

The acoustic composition/decomposition matrices also become scalars, given by

$$\tilde{\mathbf{L}}_1^\pm(z) = 1 \ , \quad \tilde{\mathbf{L}}_2^\pm(z) = \pm[q(z)/\rho(z)] \ , \tag{5}$$

and

$$\tilde{\mathbf{N}}_1^\pm(z) = ½ \ , \quad \tilde{\mathbf{N}}_2^\pm(z) = \pm[\rho(z)/2q(z)] \ , \tag{6}$$

where $\rho(z)$ is the density and $q(z)$ the vertical rayparameter, defined by

$$q(z) = \sqrt{[c^{-2}(z) - p^2]} \ , \tag{7}$$

with $c(z)$ the acoustic propagation velocity. Note that the operators depend only on the velocity and density of the acoustic medium. Substitution of equations (3-6) into equation (2) yields

$$\tilde{P}^{\pm}(z) = ½\tilde{P}(z) \pm [\rho(z)/2q(z)]\tilde{V}_z(z) \ , \tag{8}$$

where $z = z_1 - \epsilon$, $\epsilon \rightarrow 0$ for an ocean-bottom at $z = z_1$ (bear in mind that the z-axis is pointing downward).

For the 2-D elastic case we have

$$\tilde{\boldsymbol{\tau}}_z(z) = \begin{pmatrix} \tilde{\tau}_{xz}(z) \\ \tilde{\tau}_{zz}(z) \end{pmatrix}, \quad \tilde{\mathbf{V}}(z) = \begin{pmatrix} \tilde{V}_x(z) \\ \tilde{V}_z(z) \end{pmatrix} \tag{9}$$

and

$$\tilde{\mathbf{D}}^{+}(z) = \begin{pmatrix} \tilde{\Phi}^{+}(z) \\ \tilde{\Psi}^{+}(z) \end{pmatrix}, \quad \tilde{\mathbf{D}}^{-}(z) = \begin{pmatrix} \tilde{\Phi}^{-}(z) \\ \tilde{\Psi}^{-}(z) \end{pmatrix}. \tag{10}$$

Here $\tilde{\tau}_{iz}(z)$ and $\tilde{V}_i(z)$ for $i = x,z$ represent the two-way wave fields at depth level z in terms of stress and velocity components; $\Phi^{\pm}(z)$ and $\Psi^{\pm}(z)$ are the one-way wavefields in terms of downgoing and upgoing P- and S-waves and are related to the P- and S-wave potentials, according to $\Phi = \Phi^+ + \Phi^-$ and $\Psi = \Psi^+ + \Psi^-$.

At the ocean-bottom $z = z_1$ the shear-stress vanishes, whereas the normal stress is equal to minus the acoustic pressure just above the ocean-bottom. Hence, one-step decomposition is accomplished by applying equation (2) at $z = z_1 + \epsilon$, $\epsilon \rightarrow 0$, with

$$-\tilde{\boldsymbol{\tau}}_z(z_1) = \begin{pmatrix} 0 \\ \tilde{P}(z_1) \end{pmatrix}. \tag{11}$$

The elastic composition/decomposition operators are given by

$$\tilde{\mathbf{L}}_1^{\pm}(z) = c_S^2 \begin{pmatrix} \pm 2pq_P & -(c_S^{-2} - 2p^2) \\ c_S^{-2} - 2p^2 & \pm 2pq_S \end{pmatrix}, \tag{12}$$

$$\tilde{\mathbf{L}}_2^{\pm}(z) = \frac{1}{\rho} \begin{pmatrix} p & \mp q_S \\ \pm q_P & p \end{pmatrix}, \tag{13}$$

$$\tilde{\mathbf{N}}_1^{\pm}(z) = \frac{1}{2}\begin{pmatrix} \pm\frac{p}{q_P} & 1 \\ -1 & \pm\frac{p}{q_S} \end{pmatrix} \tag{14}$$

and

$$\tilde{\mathbf{N}}_2^{\pm}(z) = \frac{\mu}{2}\begin{pmatrix} 2p & \pm\frac{c_S^{-2}-2p^2}{q_P} \\ \mp\frac{c_S^{-2}-2p^2}{q_S} & 2p \end{pmatrix}, \tag{15}$$

where the P- and S-wave velocities are defined as

$$c_P = \sqrt{[(\lambda + 2\mu)/\rho]}\ , \quad c_S = \sqrt{(\mu/\rho)}\ , \tag{16}$$

(λ and μ are the Lamé coefficients) and the vertical rayparameters as

$$q_P = \sqrt{(c_P^{-2} - p^2)}\ , \quad q_S = \sqrt{(c_S^{-2} - p^2)}\ . \tag{17}$$

The elastic operators depend solely on the P- and S-wave velocity and the density just below the receiver level.

In the previously treated elastic decomposition procedure the up- and downgoing waves and the P- and S-waves were separated simultaneously. The same decomposition result can also be obtained in two steps. A derivation of the equations for multi-component surface data is given in Wapenaar and Haimé (1991). Here a similar derivation is presented for ocean-bottom data. In the two-step decomposition procedure the first decomposition step yields up- and downgoing fields expressed in terms of stresses. This choice is arbitrary; other wave field quantities could be chosen. However, with this choice the decomposition operators will appear to have a simple form. The derivation of the partial decomposition operators is as follows. From equation (1) we obtain

$$-\tilde{\boldsymbol{\tau}}_z(z_1) = \underbrace{\tilde{\mathbf{L}}_1^{+}(z_1)\tilde{\mathbf{D}}^{+}(z_1)}_{-\tilde{\boldsymbol{\tau}}_z^{+}(z_1)} + \underbrace{\tilde{\mathbf{L}}_1^{-}(z_1)\tilde{\mathbf{D}}^{-}(z_1)}_{-\tilde{\boldsymbol{\tau}}_z^{-}(z_1)}, \tag{18}$$

or

$$\begin{pmatrix} -\tilde{\boldsymbol{\tau}}_z^{+}(z_1) \\ -\tilde{\boldsymbol{\tau}}_z^{-}(z_1) \end{pmatrix} = \begin{pmatrix} \tilde{\mathbf{L}}_1^{+}(z_1) & \mathbf{O} \\ \mathbf{O} & \tilde{\mathbf{L}}_1^{-}(z_1) \end{pmatrix} \begin{pmatrix} \tilde{\mathbf{D}}^{+}(z_1) \\ \tilde{\mathbf{D}}^{-}(z_1) \end{pmatrix}, \tag{19}$$

or, upon substitution of equation (2)

$$\begin{pmatrix} -\tilde{\boldsymbol{\tau}}_z^{+}(z_1) \\ -\tilde{\boldsymbol{\tau}}_z^{-}(z_1) \end{pmatrix} = \begin{pmatrix} \tilde{\mathbf{M}}_1^{+}(z_1) & \tilde{\mathbf{M}}_2^{+}(z_1) \\ \tilde{\mathbf{M}}_1^{-}(z_1) & \tilde{\mathbf{M}}_2^{-}(z_1) \end{pmatrix} \begin{pmatrix} -\tilde{\boldsymbol{\tau}}_z(z_1) \\ \tilde{\mathbf{V}}(z_1) \end{pmatrix}, \tag{20}$$

where the partial decomposition operators are defined as

$$\tilde{\mathbf{M}}_1^{\pm}(z_1) = \tilde{\mathbf{L}}_1^{\pm}(z_1)\tilde{\mathbf{N}}_1^{\pm}(z_1) \ , \tag{21}$$

$$\tilde{\mathbf{M}}_2^{\pm}(z_1) = \tilde{\mathbf{L}}_1^{\pm}(z_1)\tilde{\mathbf{N}}_2^{\pm}(z_1) \ . \tag{22}$$

For the second decomposition step into P- and S-waves equation (19) is merely inverted, yielding

$$\begin{pmatrix} \tilde{\mathbf{D}}^+(z_1) \\ \tilde{\mathbf{D}}^-(z_1) \end{pmatrix} = \begin{pmatrix} \{\tilde{\mathbf{L}}_1^+(z_1)\}^{-1} & \mathbf{O} \\ \mathbf{O} & \{\tilde{\mathbf{L}}_1^-(z_1)\}^{-1} \end{pmatrix} \begin{pmatrix} -\tilde{\boldsymbol{\tau}}_z^+(z_1) \\ -\tilde{\boldsymbol{\tau}}_z^-(z_1) \end{pmatrix} . \tag{23}$$

Expressions for the two-step decomposition operators of the first step for the 2-D case can then be obtained by substituting equations (21), (22) and (12)-(15) into equation (20). We find

$$-\tilde{\boldsymbol{\tau}}_z^{\pm}(z_1) = -\tilde{\mathbf{M}}_1^{\pm}(z_1)\tilde{\boldsymbol{\tau}}_z(z_1) + \tilde{\mathbf{M}}_2^{\pm}(z_1)\tilde{\mathbf{V}}(z_1) \ , \tag{24}$$

or

$$\begin{pmatrix} -\tilde{\tau}_{xz}^{\pm}(z_1) \\ -\tilde{\tau}_{zz}^{\pm}(z_1) \end{pmatrix} = \frac{1}{2} \begin{pmatrix} 1 & \pm\frac{\gamma p}{q_S} \\ \mp\frac{\gamma p}{q_P} & 1 \end{pmatrix} \begin{pmatrix} 0 \\ \tilde{P}(z_1) \end{pmatrix} + \frac{\rho}{2} \begin{pmatrix} \pm\frac{\beta}{q_S} & 0 \\ 0 & \pm\frac{\beta}{q_P} \end{pmatrix} \begin{pmatrix} \tilde{V}_x(z_1) \\ \tilde{V}_z(z_1) \end{pmatrix} , \tag{25}$$

or

$$-\tilde{\tau}_{xz}^{\pm}(z_1) = \pm(\gamma p/2q_S)\tilde{P}(z_1) \pm (\rho\beta/2q_S)\tilde{V}_x(z_1) \ , \tag{26}$$

$$-\tilde{\tau}_{zz}^{\pm}(z_1) = \tfrac{1}{2}\tilde{P}(z_1) \pm (\rho\beta/2q_P)\tilde{V}_z(z_1) \ , \tag{27}$$

where

$$\beta = c_S^4[4p^2 q_P q_S + (c_S^{-2} - 2p^2)^2] \ , \tag{28}$$

$$\gamma = c_S^2[2q_P q_S - (c_S^{-2} - 2p^2)] \ , \tag{29}$$

$$q_P = \sqrt{(c_P^{-2} - p^2)} \ , \tag{30}$$

$$q_S = \sqrt{(c_S^{-2} - p^2)} \ . \tag{31}$$

Note the simple structure of equations (26) and (27): only two data-components are required simultaneously. Also note that equation (27) has the same form as the acoustic decomposition equation (8), apart from the factor β (this factor approaches unity when c_S approaches zero).

For the P- and S-wave decomposition step, equation (12) is substituted into equation (23) to obtain

$$-\tilde{\mathbf{D}}^{\pm}(z_1) = \{\tilde{\mathbf{L}}_1^{\pm}(z_1)\}^{-1}\,\tilde{\tau}_z^{\pm}(z_1) \quad , \tag{32}$$

or

$$\begin{pmatrix} \tilde{\Phi}^{\pm}(z_1) \\ \tilde{\Psi}^{\pm}(z_1) \end{pmatrix} = \frac{c_S^2}{\beta} \begin{pmatrix} \pm 2pq_S & c_S^{-2} - 2p^2 \\ -(c_S^{-2} - 2p^2) & \pm 2pq_P \end{pmatrix} \begin{pmatrix} -\tilde{\tau}_{xz}^{\pm}(z_1) \\ -\tilde{\tau}_{zz}^{\pm}(z_1) \end{pmatrix} . \tag{33}$$

AN ADAPTIVE DECOMPOSITION SCHEME

The two-step procedure provides the possibility to apply an adaptive decomposition to ocean-bottom data without any a priori knowledge of the medium parameters below the ocean-bottom and the calibration factors between the measurements of the different components. For practical use, the proposed two-step decomposition scheme is extended to five stages. It makes use of three intermediate decomposition results. In the last stage the up- and downgoing P- and S-waves are obtained.

The adaptive decomposition scheme will be described and illustrated by means of a deep ocean-bottom field dataset. The dataset has been acquired in the Vøring area, offshore Norway and is described by Brink et al. (1996). From this dataset one receiver position at the ocean-bottom was selected where both pressure and partial velocity has been measured. This receiver position has a full coverage of 401 shots at the sea-surface, with a shot interval of approximately 25 meters, resulting for each component in a common-receiver gather of 401 traces with 25 meters spacing (Fig. 1). The frequency bandwidth of the data goes up to 60 Hz. In order to apply the theory of the previous section the common-receiver gather will be treated as a common-shot gather. Strictly speaking this assumption is correct only for a 1-D medium (reciprocity of course remains valid). Although in this dataset some structures are present deeper below the bottom, for the first package of reflectors the situation is practically 1-D. Note, however, that the necessity of using common-receiver gathers is not a limitation of the method but rather of the acquisition. When there is enough receiver coverage, common-shot gathers can be used. The error made by assuming common-receiver gathers equal to common-shot gathers when the medium is not purely 1-D, is that events will be mapped onto (slightly) wrong p-values in the rayparameter domain. This will cause additional errors in the medium parameter estimation discussed further on in stage 4. Therefore, when the medium has complex structures, common-shot gathers should be used.

The decomposition will be applied to the data of Fig. 1. To transform the data to the rayparameter-frequency domain, a temporal and 1-D spatial Fourier transform and interpolation will be used. The 1-D spatial Fourier transform as well as the previously discussed decomposition equations hold for a 2-D situation (i.e., line-source data, not point-source data). Therefore, the data amplitudes should be transformed from 3-D to 2-D geometrical spreading in advance. In a horizontally layered medium (1-D) this can be done by using lateral filter operations, as described by Wapenaar et al. (1992). They also propose to perform this amplitude correction on CMP-gathers for media that are not purely 1-D, which was not possible here by lack of data. Therefore, this dataset has been simply corrected by multiplication of the amplitudes with the square-root of time. Even without amplitude correction, it has been shown (Osen et al., 1999) that the decomposition procedure will still work reasonably well, except for high propagation angles and small source-receiver separation.

Stage 1. 'Rotation' of the velocity components

In this first stage the V_z measurement is corrected for imperfections in the acquisition that are not addressed further on in the scheme. When the measured V_z component is truly that part of the wavefield with its displacement perpendicular to the ocean-bottom, it is expected that the same events are recorded as on the P component. However, if the pressure and vertical velocity components of the field data are compared (Figs. 1a and 1b), strong events with a low moveout velocity are observed on the V_z component, e.g., in the window marked **B**, that are not present on the P component. These events (presumably converted waves) will not be compensated for when the components are combined in the decomposition procedure and therefore they will deteriorate the decomposition result if they are not removed*.

To remove the unwanted events from the V_z component, a rotation of the geophone components was attempted (assuming that the vertical component was not measuring truly perpendicular to the bottom). However, this did not give satisfying results so instead a 'cross-coupling' between the velocity components is assumed. To resolve this, the following approach is taken

$$v_z(x,t) = \hat{v}_z(x,t) - r_1(t)*\hat{v}_x(x,t) - r_2(t)*\hat{v}_y(x,t) \quad , \tag{34}$$

where $\hat{v}_i(x,t)$ for $i = x,y,z$ are the measured velocity components in the space-time domain and $r_i(t)$ for $i = 1,2$ are temporal convolution operators that need to be determined by optimization. As in the window **B** (Fig. 1) almost no

*An explanation for the occurrence of events on the V_z component that are not on the P component is that they are caused by 'mechanical cross-coupling' - a leaking of energy between the three geophone components (Maxwell, 1998).

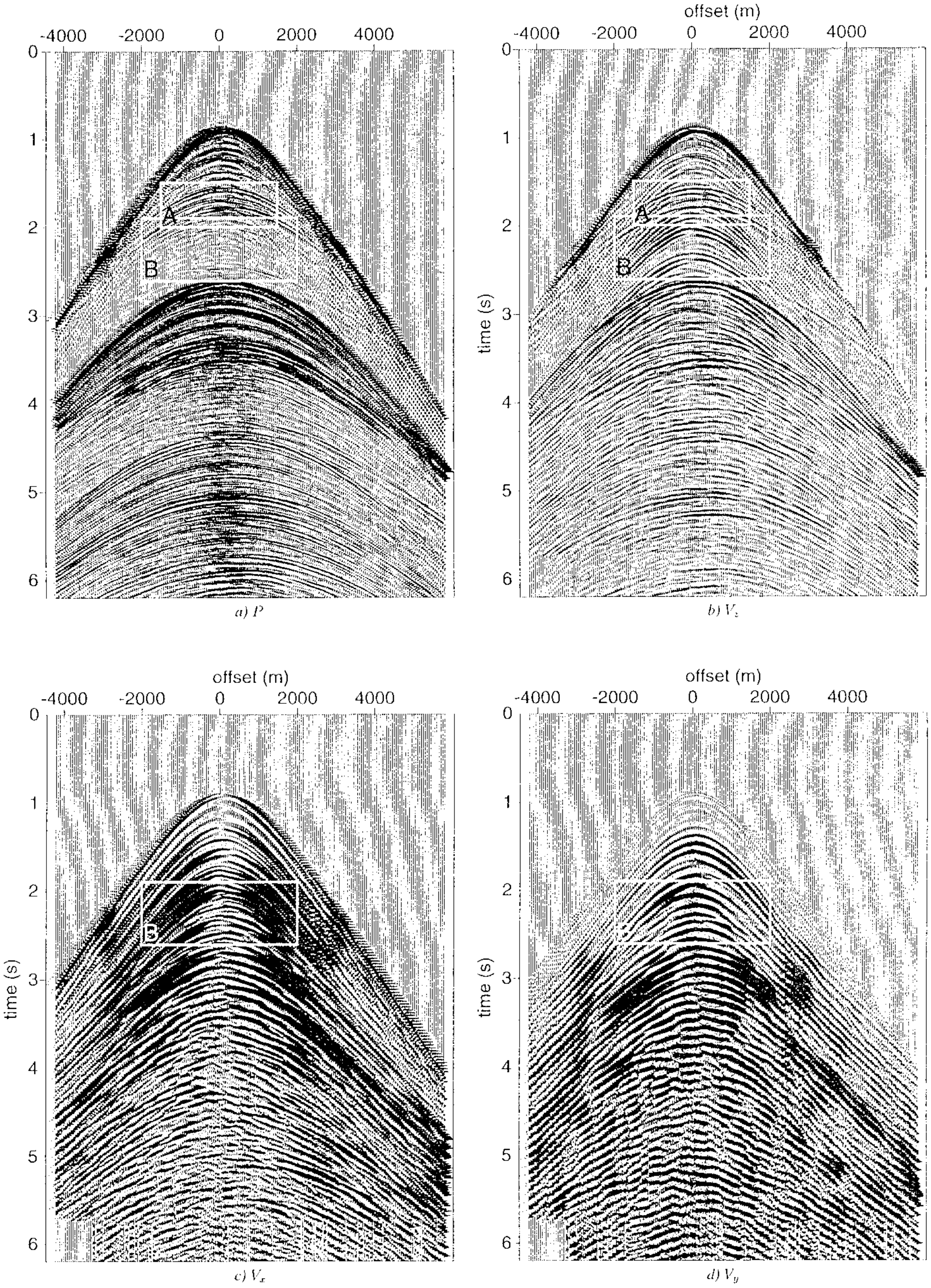

Fig. 1. Ocean bottom measurements of the Vøring dataset, provided by Saga Petroleum A.S.A., Norway. a) Pressure just above the bottom. b) Vertical component of the multi-component geophone. The windows A and B are related to the first and second stage of the adaptive decomposition scheme. c) Horizontal inline component of the multi-component geophone. d) Horizontal crossline component of the multi-component geophone.

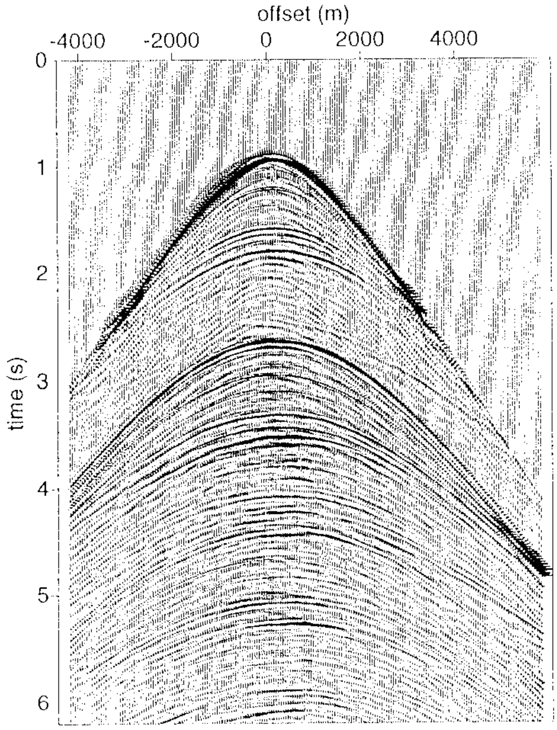

Fig. 2. Output of stage 1 of the adaptive decomposition scheme; V_z after correcting for 'cross-coupling'.

energy is arriving on the P component, the convolution filters were calculated to minimize the energy over this window on the V_z component. The resulting V_z is shown in Fig. 2. In the following stages of the decomposition scheme the corrected V_z will be used.

Stage 2. Acoustic decomposition just above the bottom

The acoustic decomposition is used to resolve the calibration filter $a(\omega)$ between the pressure and vertical velocity component:

$$\tilde{P}^{\pm} = \tfrac{1}{2}\tilde{P} \pm a(\omega)(\rho_1/2q_1)\tilde{V}_z \ , \tag{35}$$

where ρ_1 and q_1 are the density and vertical slowness in the water-layer. The calibration filter is supposed to include all differences between the hydrophone and the vertical geophone component that are not related to the actual wavefield propagation, e.g. differences in coupling and impulse response of the measuring devices. The acoustic decomposition operators are already known (as they depend solely on the velocity and density of the water), leaving $a(\omega)$ as the only unknown factor. To resolve $a(\omega)$ the extra condition is imposed that there should be no primary reflections present in the decomposed downgoing wavefield *above* the bottom (P^+).

In the field data a window **A** is chosen that contains mainly primary reflections (see Figs. 1a and 1b). The calibration filter $a(\omega)$ is calculated that best minimizes the energy in window **A** in the decomposed *downgoing* wavefield. The acoustic decomposition result is shown in Fig. 3. All primary reflection energy has been moved to the upgoing wavefield. Note that the energy of the multiples (arriving at the zero-offset channel from approximately 2.6 seconds) has been decreased in the upgoing wavefield. The summation of the two decomposed wavefields will yield again the total pressure of Fig. 1a ($P = P^+ + P^-$).

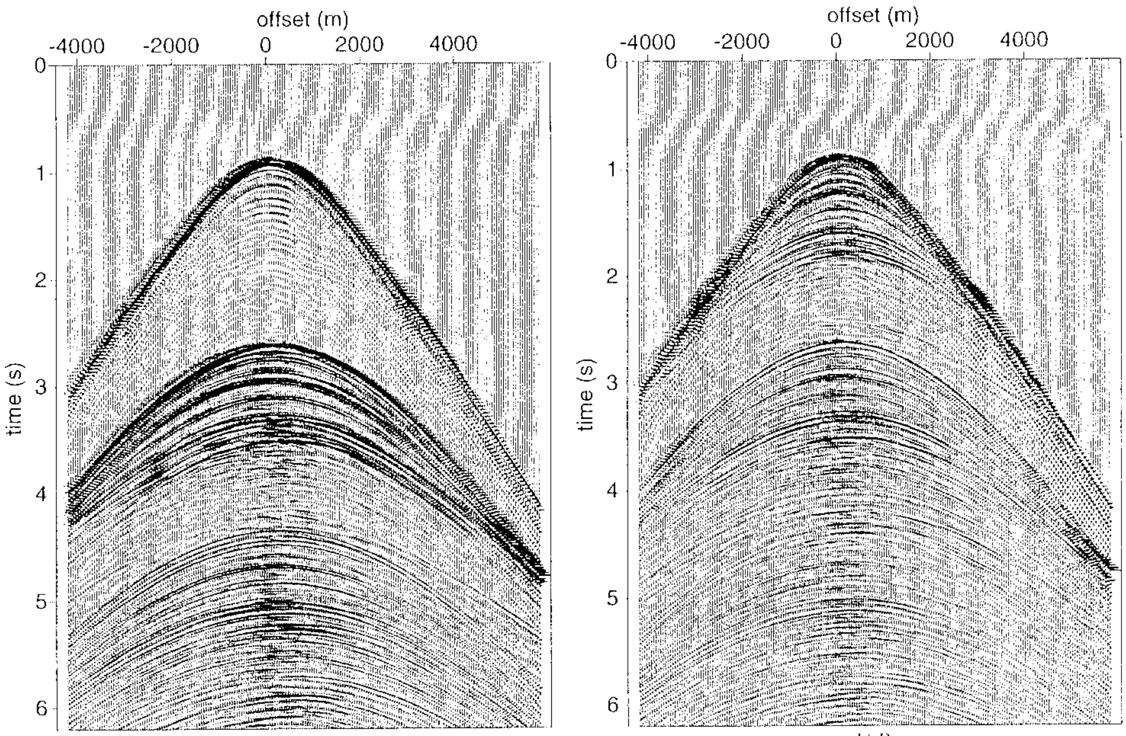

a) P^+ b) P^-

Fig. 3. Output of stage 2 of the adaptive decomposition scheme. a) Downgoing pressure wavefield just above the bottom. b) Upgoing pressure wavefield just below the bottom.

Stage 3. Elastic decomposition into $\tau^{\pm}_{zz}$ just below the bottom

The next stage is an elastic decomposition *below* the bottom, into up- and downgoing normal stressfields. As in the previous stage we are dealing again with the P and V_z components:

$$-\tilde{\tau}^{\pm}_{zz} = \tfrac{1}{2}\tilde{P} \pm a(\omega)(\rho_2\beta_2/2q_{P,2})\tilde{V}_z \quad , \tag{36}$$

where ρ_2 and $q_{P,2}$ are the density and vertical P-wave slowness of the medium just below the bottom.

The calibration filter $a(\omega)$ is already known from stage 2. This time the unknown factor is the operator in front of the V_z component, as it depends on the (unknown) medium parameters just below the bottom. To find the operator, the expression is replaced by a general rayparameter dependent filter $f(p)$:

$$-\tilde{\tau}^{\pm}_{zz} = \tfrac{1}{2}\tilde{P} \pm \mathrm{a}(\omega)f(p)\tilde{V}_z \quad . \tag{37}$$

The condition imposed on the decomposition result is that there should be no direct wave and water bottom multiples in the upgoing normal stressfield *below* the bottom.

The decomposition results of the third stage are shown in Figs. 4a and 4b. The energy minimization was done in two curved windows over the direct wave and the first-order multiple in $\tilde{\tau}^{-}_{zz}$ in the rayparameter-frequency domain. The direct arrival has been well removed, as well as the first order water multiple. In fact all surface-related multiples should be removed from the upgoing stressfield, except the source-side peg-leg multiples*.

Stage 4. Elastic decomposition into $\tau^{\pm}_{xz}$ just below the bottom

The fourth decomposition stage involves the P and $\tilde{V}_x$ components, making it possible to resolve the calibration filter $b(\omega)$ between them:

$$-\tilde{\tau}^{\pm}_{xz} = \pm(\gamma_2 p/2q_{S,2})\tilde{P} \pm b(\omega)(\rho_2\beta_2/2q_{S,2})\tilde{V}_x \quad , \tag{38}$$

From equation (38) we can see that first the decomposition operators need to be calculated with the medium parameters just below the ocean-bottom, before $b(\omega)$ can be obtained. An estimate of the medium parameters can be obtained by inverting the filter $f(p)$ found previously. The amplitude of the decomposition operator takes on the value of the P-wave impedance for normal

*To remove these multiples as well, an additional surface-related multiple elimination procedure could be applied. However, then a full receiver coverage at the bottom is necessary.

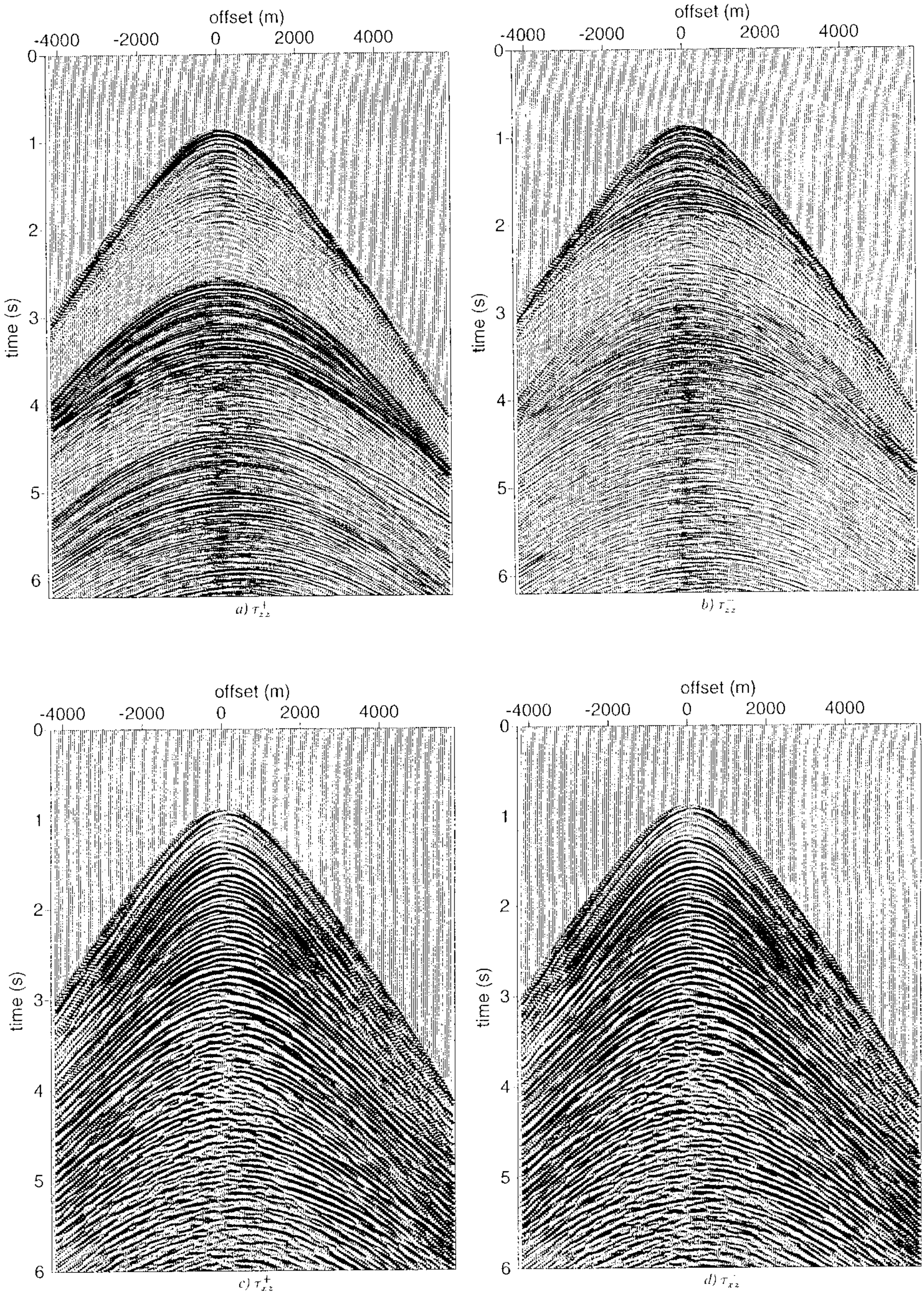

Fig. 4. Top: Output of stage 3 of the adaptive decomposition scheme. a) Downgoing normal stressfield just below the bottom. b) Upgoing normal stressfield just below the bottom. Bottom: Output of stage 4 of the adaptive decomposition scheme. c) Downgoing shear stressfield just below the bottom. d) Upgoing shear stressfield just below the bottom.

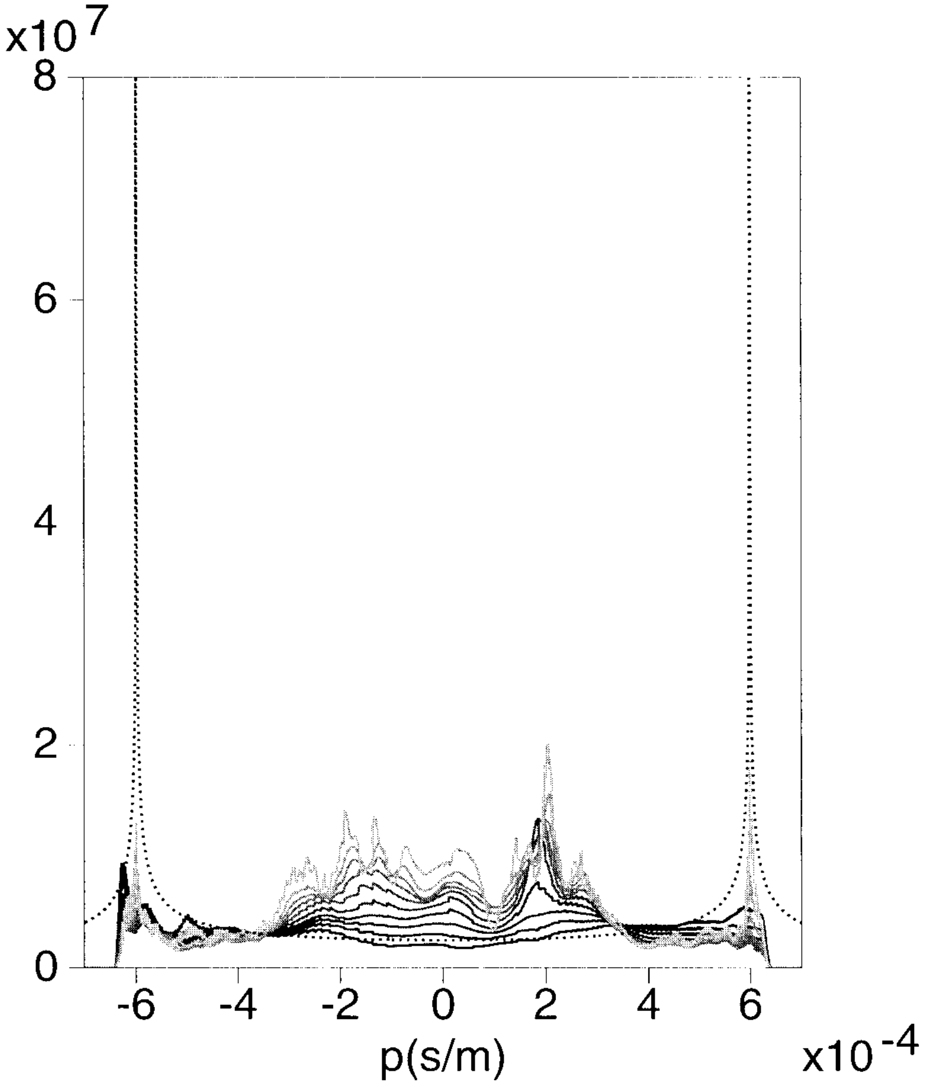

Fig. 5. The filter $f(p)$ for frequencies between 13 and 53 Hz (black to grey lines) and the modulus of the theoretical decomposition operator $\rho\beta/2q_P$ (dashed line) for c_P = 1670 m/s, c_S = 100 m/s and ρ = 1497 kg/m^3.

incidence, therefore an estimate of the impedance can be obtained from the amplitude at $p = 0$. The amplitude of the decomposition operator becomes very large when the rayparameter corresponds to the critical angle ($1/c_P$) giving an estimate for c_P. In Fig. 5, the filter $f(p)$ obtained from the data is shown for frequencies between 13 and 53 Hz (from dark to light). The modulus of the best-fitting theoretical decomposition operator is plotted in the same figure (dashed line). Note that the frequency-dependency of the filter $f(p)$ can not be explained by the theoretical operator. The average value for the impedance from Fig. 5 is $2.5\cdot10^6$ kg/m^{2}s, c_P was estimated from the peaks at $p = \pm\ 1/1670$ s/m, giving a density estimate of 1497 kg/m^3. A value for c_S could not be obtained from $f(p)$ as the post-critical angles, containing this information, were not well recorded in these data. Therefore the value for c_S was optimized in combination with the calibration filter $b(\omega)$. The condition for the optimal decomposition result is that there should be no direct wave in either the up- or downgoing shear stressfields (as both fields are equal except for an opposite polarity to satisfy the boundary condition at the ocean-bottom: $\tau_{xz} = 0$). The minimization was done over a curved window containing the direct wave, in the rayparameter-frequency domain. The value for c_S at which the direct wave was best removed was 100 m/s. The final result for the up- and downgoing shear stressfields is shown in Figs. 4c and 4d. Note that the direct wave has been attenuated but could not be completely removed. Note also that $\tau^+_{xz} = -\tau^-_{xz}$, which follows from equation (38).

Stage 5. Elastic decomposition into $\Phi^\pm$ and $\Psi^\pm$

In the last stage the estimated parameters just below the ocean-bottom and the results of the elastic decomposition into up- and downgoing stressfields are simply combined to obtain the up- and downgoing P- and S-waves:

$$\tilde{\Phi}^\pm = (c_S^2/\beta)[\mp 2pq_S\tilde{\tau}^\pm_{xz} - (c_S^{-2} - 2p^2)\tilde{\tau}^\pm_{zz}] \ , \qquad (39)$$

$$\tilde{\Psi}^\pm = (c_S^2/\beta)[(c_S^{-2} - 2p^2)\tilde{\tau}^\pm_{xz} \mp 2pq_P\tilde{\tau}^\pm_{zz}] \ . \qquad (40)$$

The results for the up- and downgoing P- and S-wave potentials are shown in Fig. 6. The results can be evaluated on the condition that there should not be any direct wave or water bottom multiples in the upgoing P- and S-waves (Figs. 6b and 6d), but cannot be changed anymore in this stage. The condition applies quite nicely to the up- and downgoing P-waves (Figs. 6a and 6b). The decomposition into S-waves (Figs. 6c and 6d) is less satisfying - very little difference is seen between the upgoing and downgoing wavefields (except for a sign change). Also, the direct wave does not seem to be much attenuated in the upgoing wavefield. The P- and (converted) S-waves appear well separated from each other. The reason for this is the low S-wave velocity just below the bottom. For this reason τ_{zz} will contain mainly P-wave energy and τ_{xz} mainly S-wave energy already.

CONCLUSIONS

A review has been given of the decomposition theory for the case of multicomponent ocean-bottom data. The process separates the P- and S-waves from each other, as well as the up- and downgoing wavefields (removing most surface-related multiples from the upgoing wavefield). In practice the decomposition equations are difficult to apply to field data, because of unknown medium parameters, coupling effects, etc.

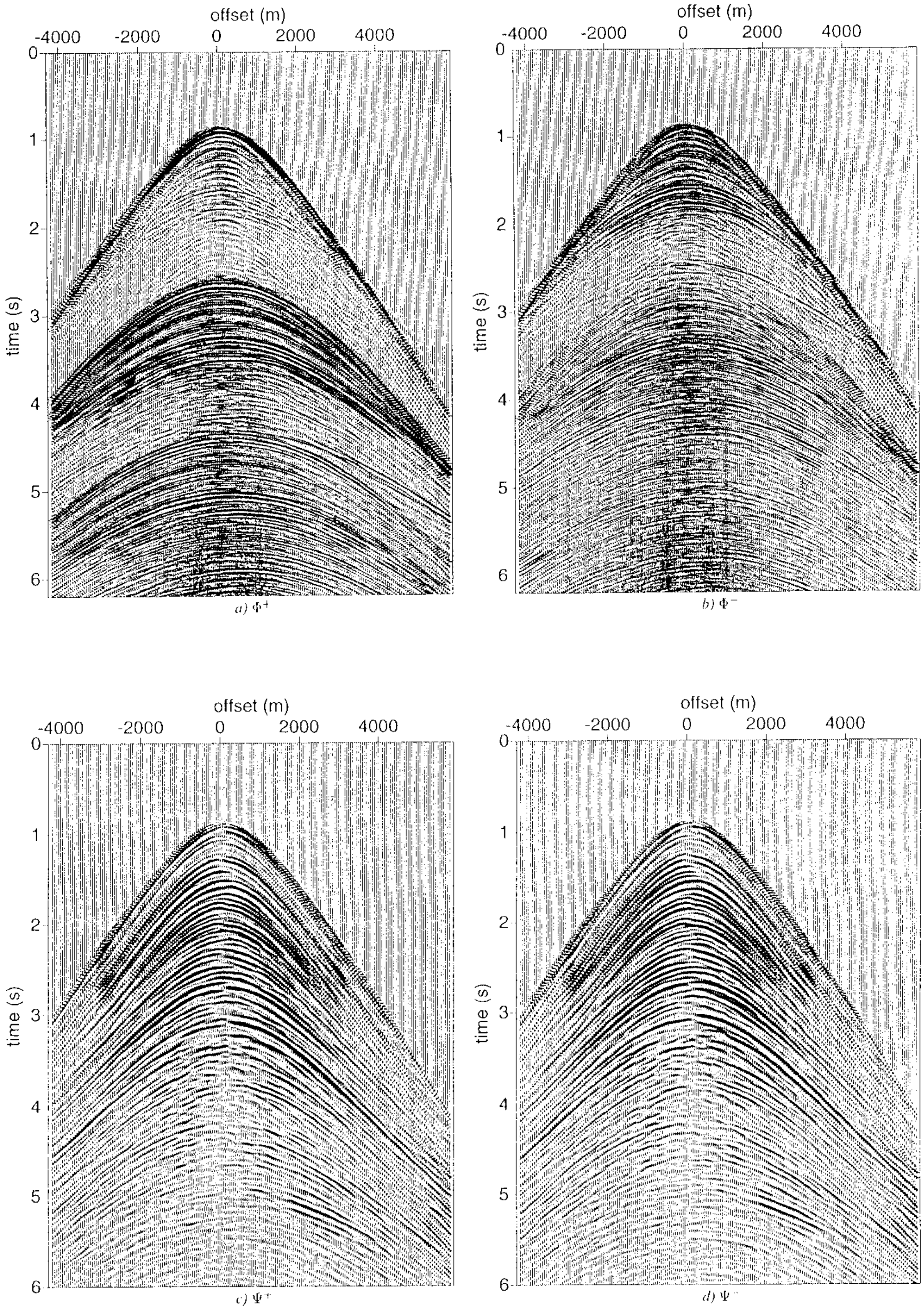

Fig. 6. Output of stage 5 of the adaptive decomposition scheme. a) Downgoing P-wave potential just below the bottom. b) Upgoing P-wave potential just below the bottom. c) Downgoing S-wave potential just below the bottom. d) Upgoing S-wave potential just below the bottom.

To facilitate application, the decomposition equations have been rewritten in a simpler form that requires less data components at a time. This result has been obtained by splitting the up- and downgoing wavefield decomposition and the P- and S-wave decomposition into two separate steps.

Based on this two-step approach, an adaptive decomposition scheme for a 2-D medium has been proposed, consisting of three intermediate decomposition results before obtaining the final result: up- and downgoing P- and S-waves. Each intermediate result allows for the estimation of some unknown parameters. In addition the quality of these results can be checked, and if necessary, improved. The scheme allows for some imperfections of the measurements (imperfect coupling of the geophones, energy leaking between the geophone components) and for unknown medium parameters just below the ocean-bottom.

The scheme has been demonstrated on a deep ocean-bottom dataset. The parameters just below the sea-floor were estimated at $c_P = 1670$ m/s, $c_S = 100$ m/s and $\rho = 1497$ kg/m^3. The decomposition results for the up- and downgoing P-waves are quite satisfactory. Moreover, P- and S-waves seem to be well separated in the final decomposition result. The separation between up- and downgoing S-waves might still be improved by also correcting the horizontal in-line geophone component for cross-coupling effects. A more precise inversion of the medium parameters of the upper part of the ocean-bottom from the estimated filter $f(p)$ will probably also benefit the result.

ACKNOWLEDGEMENTS

The authors would like to thank SAGA Petroleum A.S.A. in Norway for permission to use the dataset.

REFERENCES

Aki, K. and Richards, P.G., 1980. Quantitative Seismology. W.H. Freeman & Co., San Francisco.

Amundsen, L. and Reitan, A., 1995. Decomposition of multicomponent sea-floor data into upgoing and downgoing P- and S-waves. Geophysics, 60: 563-572.

Brink, M., Granger, P.Y., Manin, M. and Spitz, S., 1996. Seismic methodologies for a 3-components sea-floor geophone experiment on a potential flat spot in the Vøring Basin. Abstracts, 58th EAGE Conf., Amsterdam, B020.

Dankbaar, J.W.M., 1985. Separation of P- and S-waves. Geophys. Prosp., 33: 970-986.

Donati, M.S. and Stewart, R.R., P- and S-wave separation at a liquid-solid interface. J. of Seismic Explor., 5: 113-127.

Frasier, C.W., 1970. Discrete time solution of plane P-SV waves in a plane layered medium. Geophysics, 35: 197-219.

Hovem, J., Richardson, M. and Stoll, R., 1990. Shear Waves in Marine Sediments. Kluwer Academic Publishers, Dordrecht, p. 41-49.

Kennett, B.L.N., 1983. Seismic Wave Propagation in Stratified Media. Cambridge University Press, Cambridge.

Maxwell, P., 1998. Personal communication. Input/Output, Inc.,

Osen, A., Amundsen, L., Reitan, A. and Helgesen, H.K., 1996. Removal of water-layer multiples from multicomponent sea-bottom data. Expanded Abstr., 66th Ann. Internat. SEG Mtg., Denver: 1531-1534.

Osen, A., Amundsen, L. and Reitan, A., 1988. Approximate plane-wave decomposition and de-multiple processing of point source data by the 1-D Fourier transform. J. of Seismic Explor., 8: 15-25.

Schalkwijk, K.M., Wapenaar, C.P.A. and Verschuur, D.J., 1998. Decomposition of multicomponent ocean-bottom data in two steps. Expanded Abstr., 68th Ann. Internat. SEG Mtg., New Orleans: 1425-1428

Tatham, R.H. and McCormack, M.D., 1991. Multicomponent Seismology in Petroleum Exploration. Investigations in Geophysics, Vol. 6. SEG, Tulsa, OK.

Ursin, B., 1983. Review of elastic and electromagnetic wave propagation in horizontally layered media. Geophysics, 48: 1063-1081.

Wapenaar, C.P.A. and Haimé, G.C., 1991. Elastic wavefield decomposition: Before or after extrapolation? Expanded Abstr., 61st Ann. Internat. SEG Mtg., Houston: 1001-1004

Wapenaar, C.P.A., Herrmann, P., Verschuur, D.J. and Berkhout, A.J., 1990. Decomposition of multicomponent seismic data into primary P- and S-wave responses. Geophys. Prosp., 38: 633-662.

Wapenaar, C.P.A., Verschuur, D.J. and Herrmann, P., 1992. Amplitude preprocessing of single and multicomponent seismic data. Geophysics, 57: 1178-1188.

White, J.E., 1965. Seismic Waves Radiation, Transmission and Attenuation. McGraw-Hill, Inc., New York.